AD-A034 761   AIR FORCE INST OF TECH WRIGHT-PATTERSON AFB OHIO SCH--ETC F/G 22/3
              ATTITUDE STABILITY OF AN ORBITING SATELLITE CONTAINING FLEXIBLE--ETC(U)
              DEC 76   P E SANDERS

UNCLASSIFIED   GA/MC/76D-13   NL

1 OF 1
AD
A034761

END
DATE
FILMED
2-77

1.0

1.1

1.25 1.4 1.6

2.8 2.5

3.2 2.2

3.6

4.0 2.0

1.8
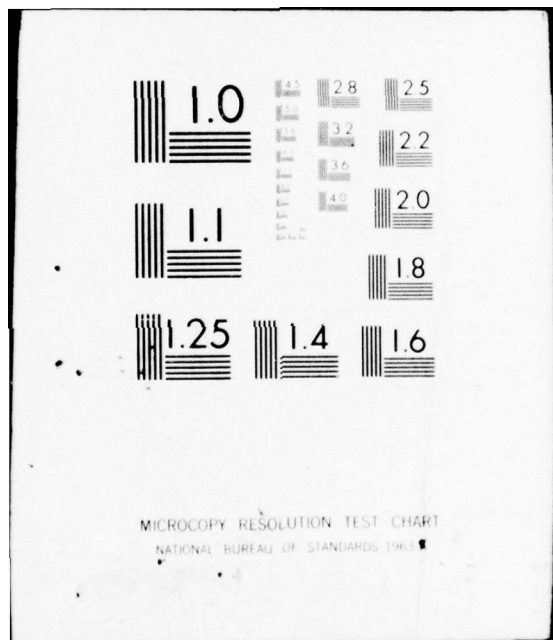
MICROCOPY RESOLUTION TEST CHART
NATIONAL BUREAU OF STANDARDS 1963

FG.

DDC
JAN 27 1977
C

UNITED STATES AIR FORCE
AIR UNIVERSITY

AIR FORCE INSTITUTE OF TECHNOLOGY

Wright-Patterson Air Force Base, Ohio

GA/MC/76D-13

DDC
RECEIVED
JAN 27 1977
C
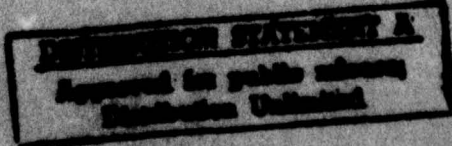
⑥

ATTITUDE STABILITY OF AN ORBITING
SATELLITE CONTAINING FLEXIBLE
ANTENNAS AND SPINNING ROTORS .

⑭ GA/MC/76D-13 THESIS ⑩ Eugene   p42
Phillip E. Sanders
Captain   USAF

⑪ Dec 76   ⑨ Master's thesis,

⑫ 51p.

012225
LB

ATTITUDE STABILITY OF AN ORBITING SATELLITE
CONTAINING FLEXIBLE ANTENNAS AND SPINNING ROTORS

THESIS

Presented to the Faculty of the School of Engineering

of the Air Force Institute of Technology

Air University

in Partial Fulfillment of the

Requirements for the Degree of

Master of Science
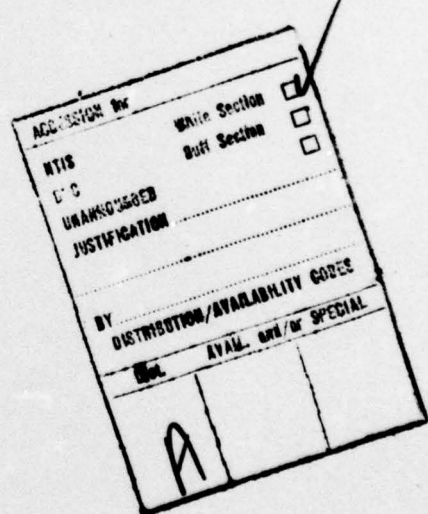
by

Phillip E. Sanders, BSE

Captain   USAF

Graduate Astronautical Engineering

December 1976

Preface

This thesis is my meager attempt to add to the body of knowledge of satellite attitude stability. Due to the immense cost of launching satellites, and having absolutely no place on earth to test stability prior to launch, only satellites which can be analyzed for stability can be built. I hope that perhaps this study may be of use to those who design satellites. If not, at least, I have learned a great deal about satellite stability and its problems.

I would like to express my thanks to my advisor, Dr. Robert A. Calico, without whose help and advice I would not have been able to complete this study.

Finally, I would like to express my very sincere gratitude and appreciation to my wife, Masae, and my son, Michael, for putting up with me during the past eighteen months.

Contents

List of Figures

Abstract

This study considers the attitude stability of a gyrostat satellite containing flexible antennas, in which any, or all, of the rotors or antennas may be misaligned with the main body principal axes. The problem is formulated in general for any number of rigid, symmetrical, spinning rotors which are fixed relative to the body and for any number of antennas, modeled as rigid rods connected by torsional springs. The stability analysis is based on the Liapunov direct method, using the Hamiltonian as the Liapunov function. Examples are presented for a gravity-stabilized satellite containing one constant-speed rotor and two antennas of two rods each. The antenna misalignment and motion is restricted to the xz plane. Results show that for a rotor misalignment, the largest deviation from the position defined by the body principal axes aligning with the orbital axes occurs when the misalignment is toward the orbit tangent. Misalignment of the antennas had no effect on the body equilibrium position except when the rotor was also misaligned. In that case, the body equilibrium angles were reduced.

ATTITUDE STABILITY OF AN ORBITING SATELLITE
CONTAINING FLEXIBLE ANTENNAS AND SPINNING ROTORS

I. Introduction

Background

The increasingly complex configurations of the earth-
orbiting satellites have generated substantial investigation
of satellite attitude stability. Results of this research
provide several useful analytical methods and several dif-
ferent models which may be used to determine stability.
Pringle (ref 1) applied Liapunov's direct method to determine
the stability of a satellite with connected moving parts.
Meirovitch and Nelson (ref 2) used an infinitesmal analysis
on a satellite containing elastic parts by assuming normal
modes of elastic displacement. Nelson and Meirovitch (ref 3)
also applied Liapunov's direct method to a satellite with
elastically connected moving parts by assuming a lumped-para-
meter representation of the distributed elastic system.
Likins (ref 4) made a study of "dual-spin" satellites con-
taining a spring-mass-damper system in the despun portion of
the satellite. Crespo da Silva (ref 5) and Rumiantsev (ref 6)
studied satellites containing internal rotors. Rumiantsev's
study was slightly more general; however, Crespo da Silva
presented results which were both more extensive and in a more
useful form. More recently, Meirovitch and Calico (ref 7)
presented an elegant method to determine stability of a satellite

1

containing flexible appendages. They used Liapunov's direct method, used the Hamiltonian as a Liapunov functional, and defined integral coordinates to evaluate the Hamiltonian. Calico (ref 8,9) extended this study to include that of Crespo da Silva to determine stability of a satellite containing both flexible appendages and internal rotors. These references are but a few of the numerous studies of satellite attitude stability which are pertinant to this study.

Each of these studies has one common characteristic; the stability was investigated about a nominal equilibrium position defined by the orbit normal and the body angular momentum vectors being aligned with a body principal moment-of-inertia axis. That is not so surprising, for generally, that particular position is the one of primary importance, and if it is not stable, the satellite is considered unstable. In these studies it was generally assumed that small misalignment errors in the rotors or antennas do not affect stability. However, what would happen to stability if misalignment were substantial, e.g., an extendable antenna failed to extend causing a rotation of the principal moments of inertia?

The Problem

The problem, then, and the purpose of this thesis is to determine the stability of a satellite containing both flexible antennas and spinning rotors, any, or all, of which could be misaligned with the body principal axes.

The General Approach

The method used by Calico will be used here, i.e.,

2

Liapunov's direct method with the Hamiltonian serving as the Liapunov function. The potential and kinetic energies were determined in general for any number of rotors and antennas, and the Hamiltonian was formulated and evaluated for sign definiteness about an equilibrium position. For the specific example presented, the equilibrium positions were found by setting the partial derivatives of the dynamic potential with respect to the generalized coordinates equal to zero. The actual calculations of the equilibrium positions and the evaluations of the Hamiltonian were done numerically.

Organization

This thesis is organized so that long mathematical derivations are not presented in the text but are included as an appendix. Also when a large set of equations exists, the entire set is included as an appendix.

II.   Mathematical Formulation of the Problem

Model and Basic Assumptions

The satellite under consideration consists of a rigid body
containing m rigid, spinning, symmetrical rotors and has attached
to it n flexible antennas. The spin axes of the rotors are fixed
relative to the main body. The antennas are modeled as a number
rigid rods connected by torsional springs. Damping in the
satellite is not modeled explicitly; however, pervasive damping
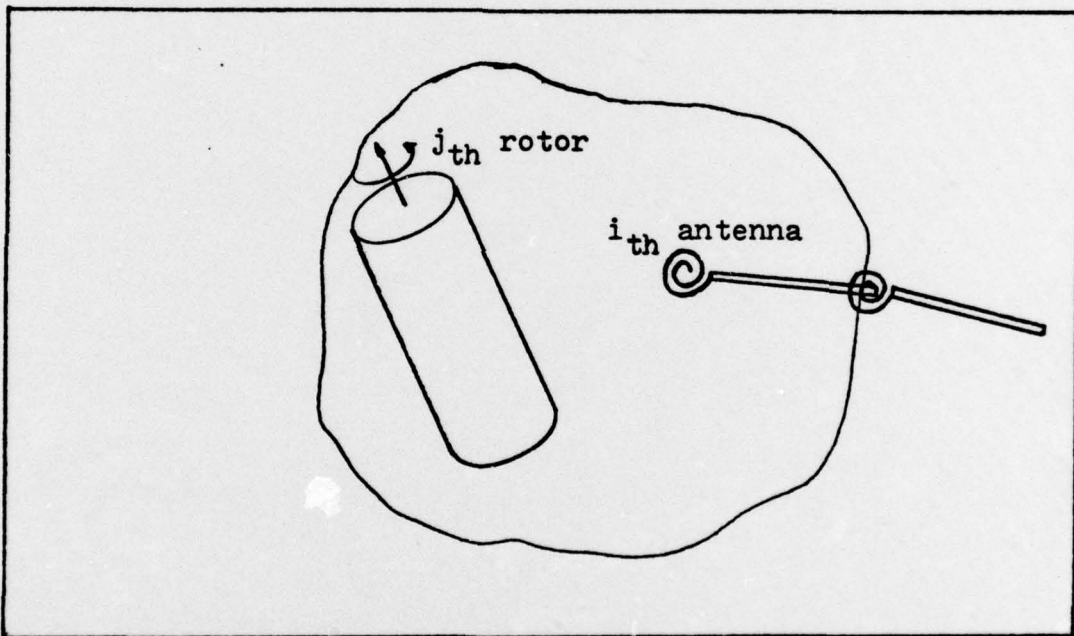
Figure 1.   The Satellite Model

will be assumed for those configurations which are otherwise
stable, thereby insuring assymptotic stability.

The earth is modeled as the central body of mass M
producing a spherically symmetric gravitational force field.
The total mass m of the satellite is small compared to M.

The last important basic assumption is that the motion
of the center of mass of the satellite is unaffected by the

4

attitude motion or the elastic motion. This assumption is
reasonable if the dimensions of the satellite are small com-
pared to the orbit radius, and the elastic motion is either
small or symmetrical about the center of mass C. This assump-
tion allows the motion of C to be calculated independently from
the attitude motion; therefore, the orbital motion is assumed
to be known. For this study, the satellite is in a circular
orbit.
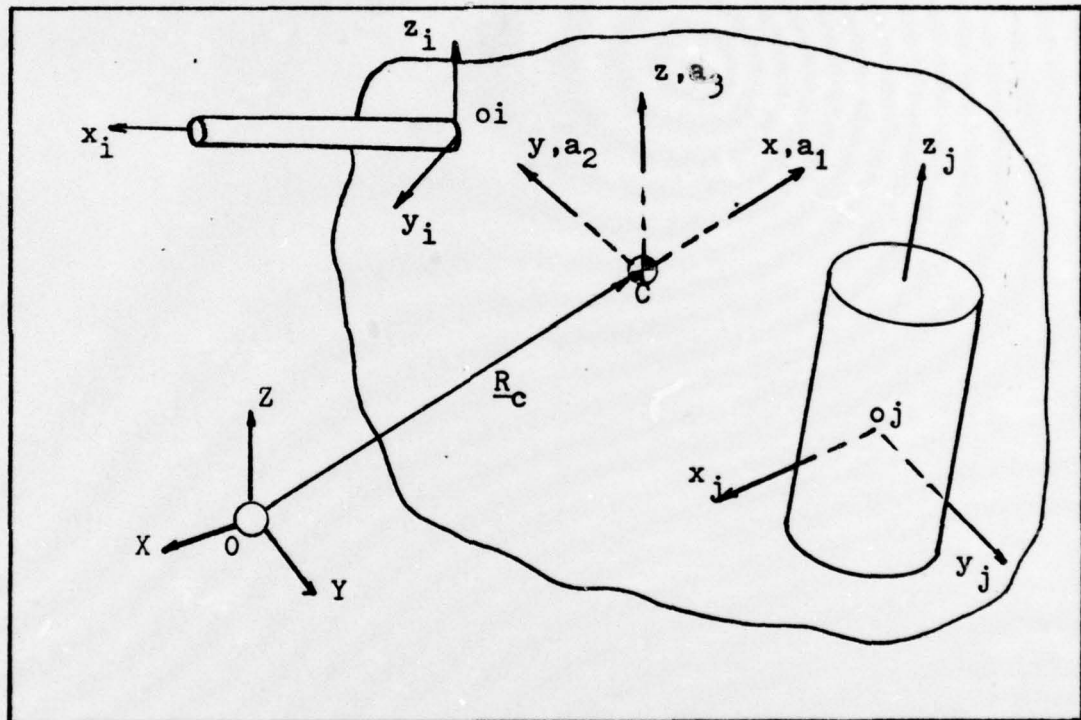
Figure 2. Coordinate Systems

Fig. 2 depicts the coordinate systems used in this thesis
The center of the earth is assumed as the origin O of an
inertial reference frame XYZ. The center of mass of the satel-
lite in its undeformed state is the origin of a set of orbital
axes $a_1 a_2 a_3$, as well as the origin of the body fixed axes xyz.
a_1 is aligned along the position vector of C in XYZ; a_2 is the

5

orbit tangent vector in the direction of the velocity vector; and a_3 is the orbit normal vector. When the satellite is undeformed, xyz represents the principal moment-of-inertia axes. $x_i y_i z_i$ define the axes for the ith antenna and are fixes with respect to xyz. They are defined such that when the antenna is undeformed it lies along one of the axes. $x_j y_j z_j$ define the nodal axes of the jth rotor such that z_j is both the symmetry axis and the spin axis. Because $x_i y_i z_i$ and $x_j y_j z_j$ are fixed in xyz, they have the same angular velocity as xyz. Although Fig. 2 shows xyz aligned with $a_1 a_2 a_3$, xyz is free to rotate. oi denotes the origin of $x_i y_i z_i$, and oj denotes the origin of $x_j y_j z_j$. (Throughout this thesis the subscripts "i" denote quantities referred to the antennas, and "j" denote quantities referred to the rotors. The subscript "o" refers to the main body. "i" numbers from 1 to n, and "j" numbers from n+1 to n+m.)

Fig. 3 depicts the position vectors and their components. Vector quantities are indicated by an underline, and their magnitudes are denoted by the same symbol without the underline, e.g., $\underline{R}_c$ is the position vector of C in XYZ, and R_c is its magnitude. Time derivatives in inertial space are denoted by a dot above the quantity, e.g., $\underline{\dot{r}}$ is the time derivative of $\underline{r}$ in inertial space. Time derivatives in the xyz frame are denoted by a dot above the quantity quantity and a prime superscript, e.g., $\underline{\dot{r}}'$ is the time derivative of $\underline{r}$ in the xyz frame.

The System Hamiltonian

To formulate the Hamiltonian of a dynamic system, the

6
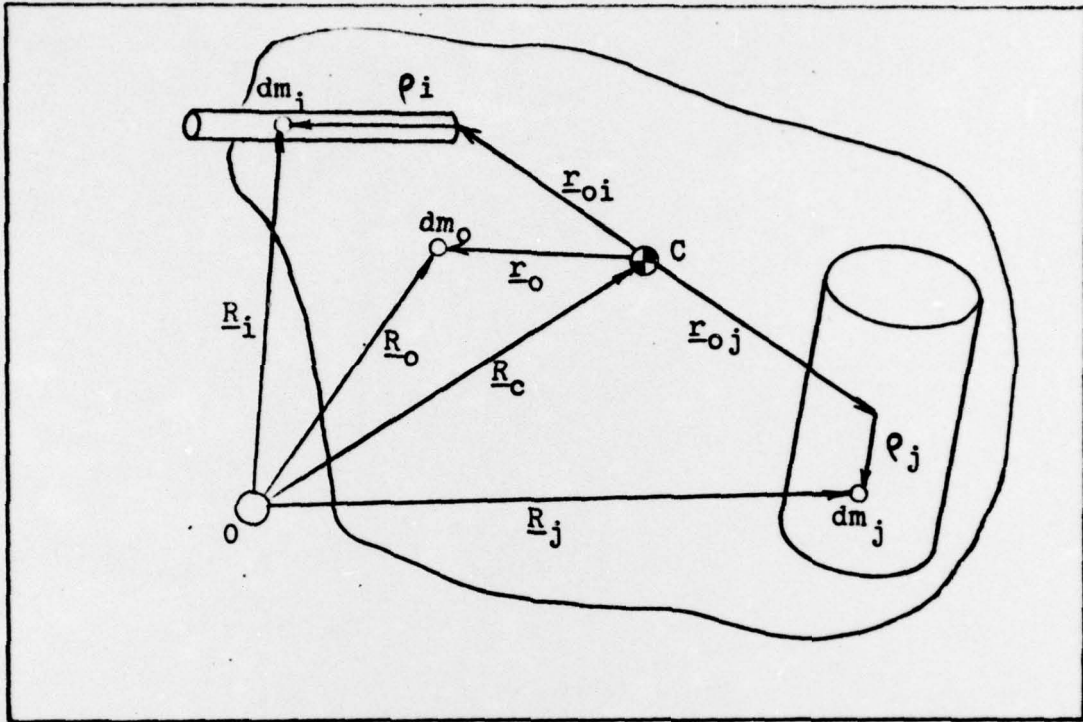
Figure 3. Position Vectors

potential and kinetic energies must be determined. The poten-
tial energy will be determined first. Meirovitch (ref 10:435)
developes the gravitational potential for a non-uniform body
in a central force field. To a second order approximation

$$V_g = -\frac{GMm}{R} - \frac{GM}{4R^3}\left[(3l^2-1)(I_{yy} + I_{zz} - I_{xx})\right.$$

$$+ (3m^2-1)(I_{xx} + I_{zz} - I_{yy}) + (3n^2-1)(I_{xx} + I_{yy} - I_{zz})$$

$$\left. + 12(lm\,I_{xy} + ln\,I_{xz} + mn\,I_{yz})\right]$$

$$\tag{1}$$

where l, m, and n are direction cosines between xyz and $\underline{R}_c$,
I_{xx}, I_{yy}, I_{zz}, ... are moments and products of inertia of the

7

of the satellite, and G is the universal gravitational constant.
The total gravitational potential of the satellite is the sum of
the potential of each part. Summing over the body and rewriting
eqn (1) in matrix form

$$V_g = -\frac{GMm}{R_c} - \frac{3GM}{2R_c^3} \sum_{i=0}^{n} tr([\ell_i]^T [J_i][\ell_i])$$

$$- \frac{3GM}{2R_c^3} \{\ell a_1\}^T (\sum_{i=0}^{n} [\ell_i]^T [J_i][\ell_i]) \{\ell a_1\} \qquad (2)$$

where $[\ell_i]$ is the direction cosine matrix between $x_i y_i z_i$ and
xyz, $[J_i]$ is the inertia matrix of the ith antenna in its
deformed state, and $\{\ell a_1\}$ is the direction cosine matrix
between R_c and xyz. The elastic potential is somewhat easier
to write:

$$V_e = \frac{1}{2} \sum_{i=1}^{n} \sum_{k=1}^{q} K_{ik} \nu_{ik}^2 \qquad (3)$$

where K_{ik} is the spring constant of the kth spring of the ith
antenna, and ν_{ik} is the angle through which the spring is
displaced from its undeformed position. Thus the total
potential is

$$V = V_g + V_e \qquad (4)$$

The kinetic energy can be written as

$$T = \frac{1}{2} \int_m \{\dot{R}\}^T \{\dot{R}\} dm \qquad (5)$$

where $\{\dot{R}\}$ is the inertial velocity of an elemental mass dm,
and m is the mass of the body. When $\{\dot{R}\}$ is written in its

8

component terms, and the integral is divided into its several

domains D_0, D_i, and D_j the kinetic energy becomes

$$T = \frac{1}{2} m \{\dot{R}_c\}^T \{\dot{R}_c\} + \frac{1}{2} \{\omega\}^T \sum_{i=0}^{n} [l_i]^T [J_i][l_i]\{\omega\}$$

$$+ \frac{1}{2} \sum_{j=n+1}^{n+m} \{\Omega\}^T [J_j]\{\Omega\} + \frac{1}{2} \sum_{i=1}^{n} \int_{D_i} \mu_i \{\dot{\rho}_i'\}^T \{\dot{\rho}_i'\} dD_i$$

$$+ \{\omega\}^T \sum_{i=1}^{n} \int_{D_i} \mu_i [\widetilde{(r_{oi} + \rho_i)}][l_i]^T \{\dot{\rho}_i'\} dD_i \qquad (6)$$

$$+ \{\omega\}^T \sum_{j=n+1}^{n+m} [l_i]^T [J_j]\{\Omega_j\}$$

where $\{\dot{R}_c\}$ is the velocity of C; μ_i is the mass density of

the ith antenna; $\{\Omega_j\}$ is the angular velocity of the jth

rotor relative to xyz; $[\widetilde{(r_{oi} + \rho_i)}]$ is the skew-symmetric matrix

which yields the vector cross product $(\underline{r}_{oi} + \underline{\rho}_i) \times \dot{\underline{\rho}}_i'$; and $[J_j]$ is

the inertia matrix of the jth rotor relative to $x_i y_i z_i$. Eqn

(6) is derived in Appendix A.

Since the orbit is circular, R_c is constant, and

$$\frac{GM}{R_c^3} = \omega_0^2 \qquad (7)$$

where ω_0 is the orbital angular velocity. The angular velocity

$\{\omega\}$ of the xyz frame with respect to inertia is

$$\{\omega\} = \omega_0 \{l_{a_3}\} + \{\omega_i\} \qquad (8)$$

where $\{l_{a_3}\}$ is the direction cosine matrix between a_3 and xyz,

and $\{\omega_i\}$ is the angular velocity between xyz and $a_1 a_2 a_3$.

Because T and V are expressed in a rotating reference frame and the orbital velocity is constant, the system is considered non-natural, and it is explicitly independent of time. For this system the Hamiltonian assumes the form

$$H = T_2 - T_0 + V \tag{9}$$

where T_2 represents the terms in T which are quadratic in the generalized veloxities, and T_0 represents the terms in T which are independent of the generalized velocities. Substituting eqn (8) into eqn (6) and grouping terms

$$T_0 = \frac{1}{2} \omega_0^2 \{la_3\}^T \sum_{i=0}^{n} [l_i]^T [J_i][l_i]\{la_3\} \tag{10}$$

and

$$T_2 = \frac{1}{2} \{\omega_i\}^T \sum_{i=0}^{n} [l_i]^T [J_i][l_i]\{\omega_i\}$$

$$+ \frac{1}{2} \sum_{j=n+1}^{n+m} \{\Omega_j\}^T [J_j]\{\Omega_j\} + \frac{1}{2} \sum_{i=1}^{n} \int_{D_i} \mu_i \{\dot{\rho}_i'\}^T \{\dot{\rho}_i'\} d D_i$$

$$+ \{\omega_i\}^T \sum_{i=1}^{n} \int_{D_i} \mu_i [(\widetilde{r_{0i} + \rho_i})][l_i]^T \{\dot{\rho}_i'\} d D_i \tag{11}$$

$$+ \{\omega_i\}^T \sum_{j=n+1}^{n+m} [l_j]^T [J_j]\{\Omega_j\}$$

Substituting eqns (4), (10), and (11) into eqn (9) yields the Hamiltonian for any number of rotors or antennas.

$$H = \frac{1}{2} \{\omega_i\}^T \sum_{i=0}^{n} [l_i]^T [J_i][l_i]\{\omega_i\}$$

$$+ \frac{1}{2} \sum_{j=n+1}^{n+m} \{\Omega_j\}[J_j]\{\Omega_j\} + \frac{1}{2} \sum_{i=1}^{n} \int_{D_i} \mu_i \{\dot{\rho}_i'\}^T \{\dot{\rho}_i'\} d D_i \tag{12}$$

10

$$+ \{\omega_1\}^T \sum_{\iota=1}^{n} \int_{D_i} \mu_i \left[(\widetilde{r_{0i} + \rho_\iota}) \right] [\ell_i]^T \{\dot{\rho_\iota}\} dD_i$$

$$+ \{\omega_1\}^T \sum_{j=n+1}^{n+m} [\ell_j]^T [J_j] \{\Omega_j\}$$

$$- \frac{1}{2} \omega_0^2 \{\ell a_3\} \sum_{\iota=0}^{n} [\ell_i]^T [J_i] [\ell_i] \{\ell a_3\}$$

$$- \frac{GM}{R_c} - \frac{3}{2} \omega_0^2 \sum_{\iota=0}^{n} tr([\ell_i]^T [J] [\ell_i])$$

$$- \frac{3}{2} \omega_0^2 \{\ell a_1\}^T \left(\sum_{\iota=0}^{n} [\ell_i]^T [J_i] [\ell_i] \right) \{\ell a_1\}$$

$$+ \frac{1}{2} \sum_{\iota=1}^{n} \sum_{K=1}^{q} K_{iK} \Psi_{iK}$$

III. Stability Analysis

Equilibrium Position

For the satellite to be stable about an equilibrium position, H, evaluated at that position, must be positive definite. In this study, because the rotors, antennas, or both are assumed to be misaligned, the nominal equilibrium position, discussed in Chapter I, generally does not exist. Therefore, an equilibrium position, hopefully, one near the nominal position, must be found and H evaluated for sign definiteness. The Hamiltonian may be expressed as

$$H = T_2 + U \tag{13}$$

where, U, the dynamic potential, is defined as

$$U = V - T_0 \tag{14}$$

Equilibrium positions are defined by the set of equations

$$\frac{\partial U}{\partial x_i} = 0 \qquad (i = 1, n) \tag{15}$$

where x_i are the generalized coordinates and n is the number of coordinates. In general, this set of equations is non-linear, and a numerical solution is required. Once the equilibrium position is found, H may be evaluated for positive definiteness to determine stability.

Evaluation of the Hamiltonian

For H to be positive definite, only U need be evaluated because by definition T_2 is positive definite; therefore,

12

H is greater that U. Sign definiteness of U is determined by forming the matrix $[U_{ij}]$, where

$$U_{ij} \equiv \frac{\partial^2 U}{\partial x_i \partial x_j} \Big|_{equilibrium} \tag{16}$$

and applying Sylvester's criterion, i.e., for positive definiteness the determinant of each of the leading principal minors of $[U_{ij}]$ must be greater than zero. If U is positive definite, then the equilibrium position is stable, and, moreover, it is assymptotically stable when pervasive damping exists.

IV. Stability of Specific Examples

Constant Speed Rotor

In each of the specific examples, the rotor is assumed to be driven at a constant speed. Since $X_j y_j z_j$ are nodal axes, $\{\Omega_j\} = \{0 \ 0 \ s_j\}^T$, where s_j is the constant spin rate of the rotor. When this is the case, the last term in T_2 reduces to a T_1 term and a T_0 term. Since neither T_1 nor T_2 appear in U, only the T_0 term will be considered. The additional T_0 term becomes

$$\omega_0 \{la_3\}^T \sum_{j=n+1}^{n+m} [\ell_j]^T [J_j] \{\Omega_j\}$$

Therefore, T_0 for a constant speed rotor becomes

$$T_{oc} = T_0 + \omega_0 \{la_3\}^T \sum_{j=n+1}^{n+m} [\ell_j]^T [J_j] \{\Omega_j\} \tag{17}$$

For all calculations T_{oc} will be used for T_0 in eqn (14).

Examples

Three specific examples are considered. The first is a satellite containing one constant speed rotor whose spin axis is nominally aligned with the z-axis, but misalignment is allowed. The second example contains one constant speed rotor aligned with the z-axis, but it has two antennas restricted to symmetrical motion but which may be misaligned. The last example is a combination of the first two. Each antenna is modeled by two rods of length L, mass m/2, and is connected by two springs of stiffness K. The antennas are attached to the main body at a distance $\pm h_x$ in the x-direction and h_z in the z-direction. The antennas are further restricted to motion only in the xz-plane. The model is shown in Fig. B-1 in Appendix B.

14

For convenience of calculation, the $[J_i]$ matrices will be redefined as $[J_i]_r$ and $[J_i]_e$, where r denotes the undeformed state, and e denotes the change due to elastic displacements. $[J_i]_r$ and $[J_i]_e$ are developed in Appendix B. $[J_i]_r$ will then be summed with $[J_o]$ to form $[J]_r$, the inertia matrix of the entire undeformed body.

$$[J]_r = [J_o] + \sum_{i=1}^{n} [l_i]^T [J_i]_r [l_i] \tag{18}$$

By appropriately defining the principal moments-of-inertia

$$[J_o] = \begin{bmatrix} A_o & & \bigcirc \\ & B_o & \\ \bigcirc & & C_o \end{bmatrix} \tag{19}$$

and

$$\sum_{i=1}^{n} [l_i]^T [J_i]_r [l_i] = mL^2 \begin{bmatrix} I_{1r} & & \bigcirc \\ & I_{2r} & \\ \bigcirc & & I_{3r} \end{bmatrix} \tag{20}$$

where

$$I_{1r} = 2\left(\frac{h_s}{L}\right)^2$$

$$I_{3r} = 2\left(\frac{h_x}{L}\right)^2 + 4\frac{h_x}{L} + \frac{8}{3} \tag{21}$$

$$I_{2r} = I_{1r} + I_{3r}$$

The inertia matrix of the undeformed body becomes

$$[J]_r = \begin{bmatrix} A_o + mL^2 I_{1r} & & \bigcirc \\ & B_o + mL^2 I_{2r} & \\ \bigcirc & & C_o + mL^2 I_{3r} \end{bmatrix} = \begin{bmatrix} A & & \bigcirc \\ & B & \\ \bigcirc & & C \end{bmatrix} \tag{22}$$

15

Also

$$[J]_e = m L^2 \begin{bmatrix} I_{1e} & & \bigcirc \\ & I_{2e} & \\ \bigcirc & & I_{3e} \end{bmatrix} \tag{23}$$

where

$$I_{1e} = -3\frac{h_z}{L}s\phi_1 + \frac{4}{3}s^2\phi_1 + \frac{1}{3}s^2\phi_2 - \frac{h_z}{L}s\phi_2 + s\phi_1 s\phi_2$$

$$I_{3e} = 3\frac{h_x}{L}c\phi_1 + \frac{4}{3}c^2\phi_1 + \frac{1}{3}c^2\phi_2 + \frac{h_x}{L}c\phi_2 + c\phi_1 c\phi_2 - \frac{8}{3} - 4\frac{h_x}{L} \tag{24}$$

$$I_{2e} = I_{1e} + I_{3e}$$

For the single rotor, define $[J_3]$ and $\{\Omega_3\}$.

$$[J_3] = \begin{bmatrix} I & & \bigcirc \\ & I & \\ \bigcirc & & J \end{bmatrix} \tag{25}$$

$$\{\Omega_3\}^T = \{0 \quad 0 \quad s\} \tag{26}$$

With the inertia matrices defined, and the rotor speed defined, the direction cosine matrices must be expressed explicitly to enable U to be calculated.

For a set of Euler angles defined by a θ_2 rotation about y, a $-\theta_1$ rotation about x, and a θ_3 rotation about z, $\{la_1\}$ and $\{la_3\}$ become

$$\{la_1\} = \begin{Bmatrix} c\theta_2 c\theta_3 - s\theta_1 s\theta_2 s\theta_3 \\ -(c\theta_2 s\theta_3 + s\theta_1 s\theta_2 c\theta_3) \\ c\theta_1 s\theta_2 \end{Bmatrix} \tag{27}$$

$$\{la_3\} = \begin{Bmatrix} -(s\theta_2 c\theta_3 + s\theta_1 c\theta_2 s\theta_3) \\ s\theta_2 s\theta_3 - s\theta_1 c\theta_2 c\theta_3 \\ c\theta_1 c\theta_2 \end{Bmatrix}$$

16

Also

$$[l_0] = [l_1] = \begin{bmatrix} \diagdown 1 \diagdown \end{bmatrix}$$

$$[l_2] = \begin{bmatrix} -1 & & 0 \\ 0 & -1 & \\ & & 1 \end{bmatrix}$$

$$[l_3] = \begin{bmatrix} c\alpha_2 & s\alpha_2 & 0 \\ -c\alpha_1 s\alpha_2 & c\alpha_1 c\alpha_2 & -s\alpha_1 \\ -s\alpha_1 s\alpha_2 & s\alpha_1 c\alpha_2 & c\alpha_1 \end{bmatrix} \tag{28}$$

where α_2 is a rotation about z_3 and $-\alpha_1$ is a rotation about x_3.

Substituting eqns (2),(3),(7),(10), and (17) into eqn (14), dividing by $C\omega_0^2$, and performing the indicated matrix operations yields the scalar equation for U_c.

$$U_c = -\frac{R_c^2}{C} - \frac{(A+B+C)}{2C} + \frac{3}{2}\left[(c\theta_2 c\theta_3 - s\theta_1 s\theta_2 s\theta_3)^2 \frac{(A+mL^2 I_{1e})}{C}\right.$$

$$\left. + (c\theta_2 s\theta_3 + s\theta_1 s\theta_2 c\theta_3)^2 \frac{(B+mL^2 I_{2e})}{C} + (c\theta_1 s\theta_2)^2 \frac{(C+mL^2 I_{3e})}{C}\right]$$

$$+ \frac{1}{2}\left[-(s\theta_2 c\theta_3 + s\theta_1 c\theta_2 s\theta_3)^2 \frac{(A+mL^2 I_{1e})}{C}\right.$$

$$- (s\theta_2 s\theta_3 - s\theta_1 c\theta_2 c\theta_3)^2 \frac{(B+mL^2 I_{2e})}{C} \tag{29}$$

$$\left. - (c\theta_1 c\theta_2)^2 \frac{(C+mL^2 I_{3e})}{C}\right] - \beta\left[(s\theta_2 c\theta_3 + s\theta_1 c\theta_2 s\theta_3)s\alpha_1 s\alpha_2\right.$$

$$\left. + (s\theta_2 s\theta_3 - s\theta_1 c\theta_2 c\theta_3)s\alpha_1 c\alpha_2 + c\theta_1 c\theta_2 c\alpha_1\right]$$

$$+ \frac{mL^2 \lambda^2}{.68C\,\omega_0^2}\left(\phi_1^2 - \phi_1\phi_2 + \frac{\phi_2^2}{2}\right)$$

17

where $\beta = Js/C\omega_o^2$ and $\lambda^2 = .68K/mL^2$. With U_c determined, a computer program was designed to evaluate the equilibrium equations and to test the sign definiteness of $[U_{ij}]$. The equilibrium equations and U_{ij} are listed in Appendix C.

In addition to β, λ^2/ω_o^2, α_1, and α_2, the following parameters were defined.

$$K_1 = (C-B)/A$$
$$K_2 = (C-A)/B$$
$$HX = h_x/L$$
$$HZ = h_z/L$$
$$RA = mL^2 I_{3r}/A_o$$

Stability was tested for various values of α_1, α_2, β, λ^2/ω_o^2, HX, HZ, RA, K_1, and K_2. K_1 and K_2 were varied throughout the region indicated in Fig. 4 by the diagonal lines. Crespo da Silva and Calico found the regions of stability for the nominal equilibrium position to lie within this area.
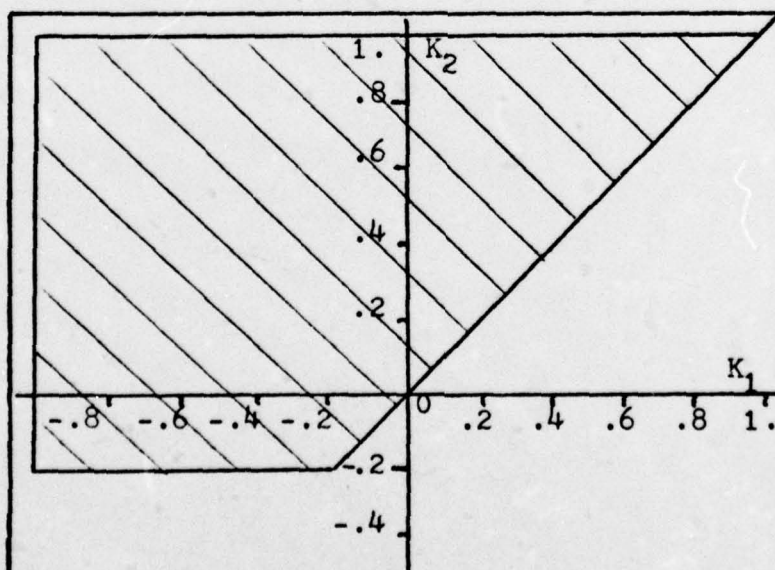

Figure 4. $K_1 K_2$ Search Region

18

Results

Obviously there are numerous solutions to the equilibrium equations; however, only the stable equilibrium positions near the nominal position are considered.

Example I. For the first example RA=0; therefore, the only parameters which were varied were K_1, K_2, β, α_1, and α_2. When $\alpha_1 = \alpha_2 = 0$, i.e., when there is no misalignment of the rotor, the results duplicate those of Crespo da Silva for the derivation is identical. However, when α_1 does not equal zero, the nominal equilibrium position no longer exists. It is interesting to note that the stable equilibrium is still defined by the angular momentum vector and the orbit normal vector aligning; however, they are no longer aligned with a body principal axis. This is easily demonstrated for the simple case where $\alpha_2 = -90^\circ$. For this case the equilibrium equation reduces to

$$\left(\frac{C-A}{C}\right) s\theta_2 c\theta_2 + \beta (c\theta_2 s\alpha_1 + s\theta_2 c\alpha_1) = 0 \tag{30}$$

where $\theta_1 = \theta_3 = 0$. The momentum is defined by

$$\{L\} = [J]_r \{l\omega_o\} \omega_o + [l_3]^T [J_3] \{\Omega_3\} \tag{31}$$

which reduces to

$$\{L\} = \left\{ \begin{array}{c} (-\omega_o A s\theta_2 c\theta_2 + \omega_o C s\theta_2 c\theta_2 + J_s s\alpha_1 c\theta_2 + J_s c\alpha_1 s\theta_2) \\ \\ 0 \\ \\ (\omega_o A s^2\theta_2 - \omega_o C c^2\theta_2 + J_s c\alpha_1 c\theta_2 + J_s s\alpha_1 s\theta_2) \end{array} \right\} \tag{32}$$

19

The first term in eqn (32) is exactly eqn (30), and all angular momentum of the equilibrium position is aligned with the orbit normal.

Fig. 5, 6, 7, and 8 show stability regions and equilibrium angle curves in the $K_1 K_2$ plane for various values of α_1, α_2 and β. For given values of α_1 and β, equilibrium angles furthest from the nominal were found to occur when $\alpha_2 = 0$, or the misalignment of the rotor was toward the a_2 axis. When misalignment was toward the a_1 axis, the equilibrium position is very near the nominal. Fig. 5, 6, and 8 also show that $\theta_{2e} = -\alpha_1$ and $\theta_{1e} = 0$ when $K_1 = 0$ or $K_2 = 1$. Fig 7 shows that $\theta_{1e} = -\alpha_1$ and $\theta_{2e} = 0$ when $K_2 = 0$. In both cases $\theta_{3e} = 0$. In fig. 5, 6, 7, and 8 the region above the solid line $K_1 = K_2$ in the first quadrant and above the solid curve in the second quadrant is the stability region for the nominal equilibrium position. In fig. 5 and 6, the region below the solid curve in the second quadrant is still stable about an equilibrium position, but the equilibrium angles become too large to be of interest. A comparison of fig. 5 and 6 shows that there is essentially no difference between the two for areas I and II; however for $\alpha_1 = 10^\circ$, area III is very slightly larger than that for $\alpha_1 = 1^\circ$. The boundary curve of area III in fig. 6 crosses the K_1 axis and $K_1 = -1$ line at nearly the same place as in fig. 5; however the curve is slightly flatter. This difference is a little more obvious in fig. 9 where θ_{1e} is plotted vs. $-\alpha_1$ for a give value of K_1, β, and α_2, and four different values of K_2, e.g., for $K_2 = .2$, $-\alpha_1 = 1^\circ$, $\theta_{1e} = 4^\circ$, and $-\alpha_1 = 10^\circ$, $\theta_{1e} = 29^\circ$. For small values of $-\alpha_1$, θ_{1e} is nearly a

20
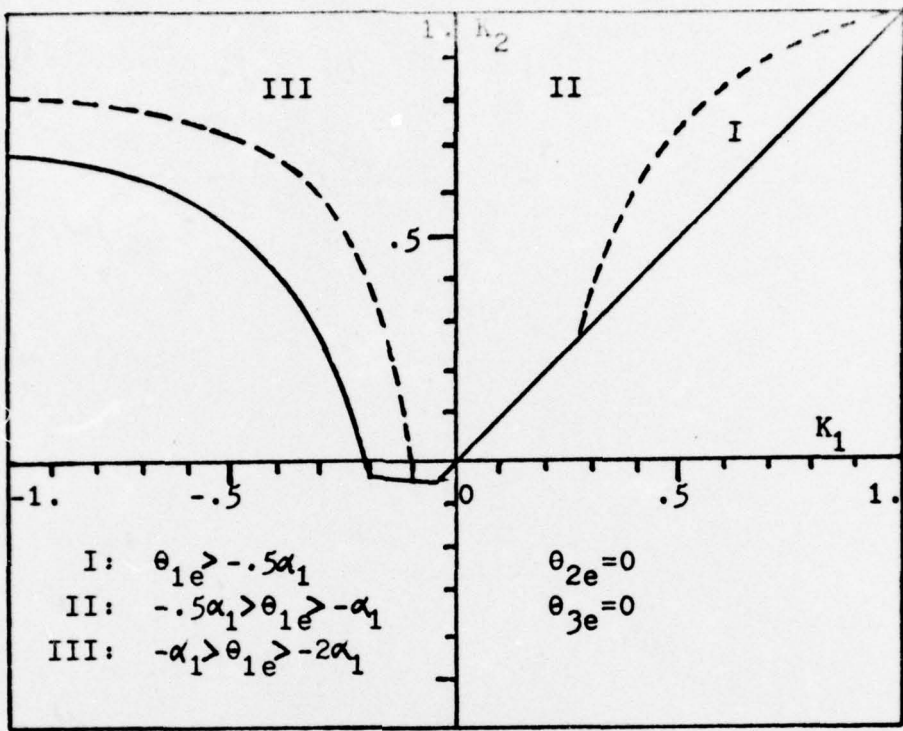
Figure 5. Stability Region and Equilibrium Angle Curves: $\alpha_1=1^\circ$, $\alpha_2=0$, $\beta=.2$, RA=0

I: $\theta_{1e} > -.5\alpha_1$

II: $-.5\alpha_1 > \theta_{1e} > -\alpha_1$

III: $-\alpha_1 > \theta_{1e} > -2\alpha_1$

$\theta_{2e}=0$

$\theta_{3e}=0$
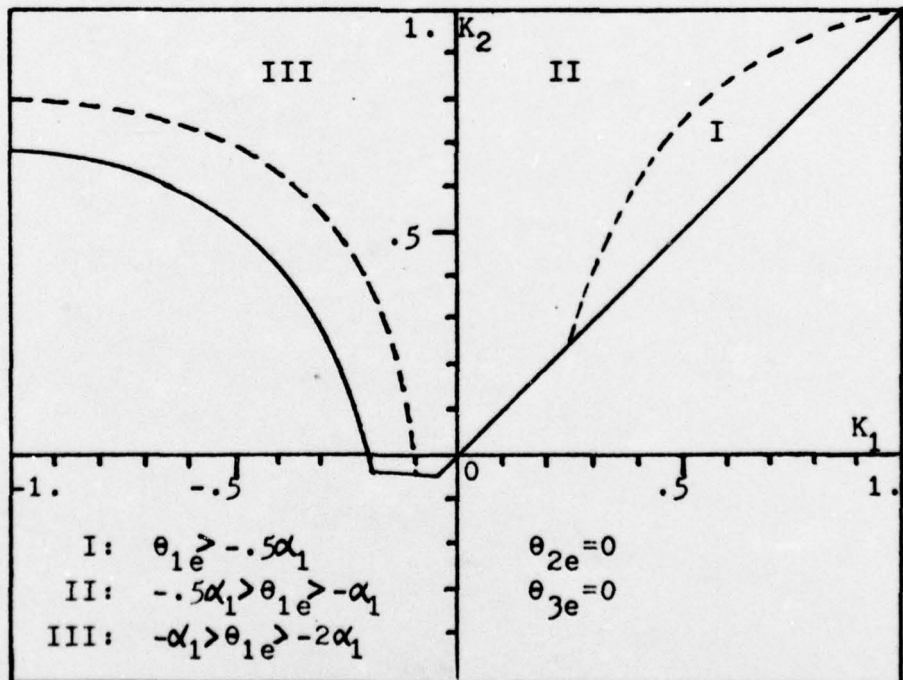
Figure 6. Stability Region and Equilibrium Angle Curves: $\alpha_1=10^\circ$, $\alpha_2=0$, $\beta=.2$, RA=0

I: $\theta_{1e} > -.5\alpha_1$

II: $-.5\alpha_1 > \theta_{1e} > -\alpha_1$

III: $-\alpha_1 > \theta_{1e} > -2\alpha_1$

$\theta_{2e}=0$

$\theta_{3e}=0$

21

I: $\theta_{2e} > -.05\alpha_1$

II: $-.05\alpha_1 > \theta_{2e} > -.1\alpha_1$

III: $-.1\alpha_1 > \theta_{2e} > -.5\alpha_1$

$\theta_{1e} = 0$
$\theta_{3e} = 0$
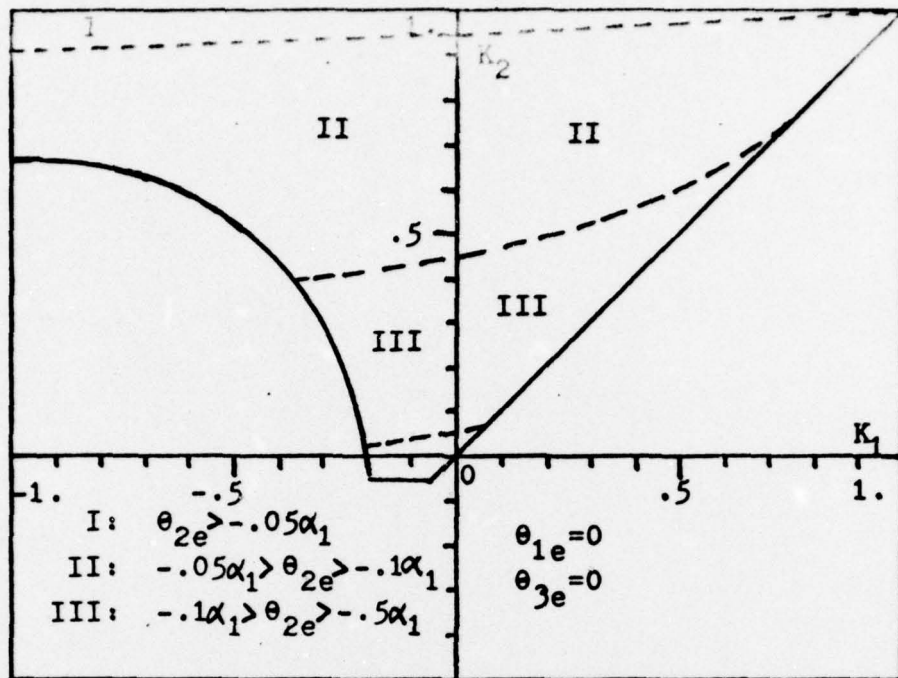
Figure 7.   Stability Region and Equilibrium Angle
Curves: $\alpha_1 = 10^\circ$, $\alpha_2 = -90^\circ$, $\beta = .2$, RA = 0

I: $\theta_{1e} > -.8\alpha_1$

II: $-.8\alpha_1 > \theta_{1e} > -\alpha_1$

III: $-\alpha_1 > \theta_{1e} > -1.5\alpha_1$

$\theta_{2e} = 0$
$\theta_{3e} = 0$
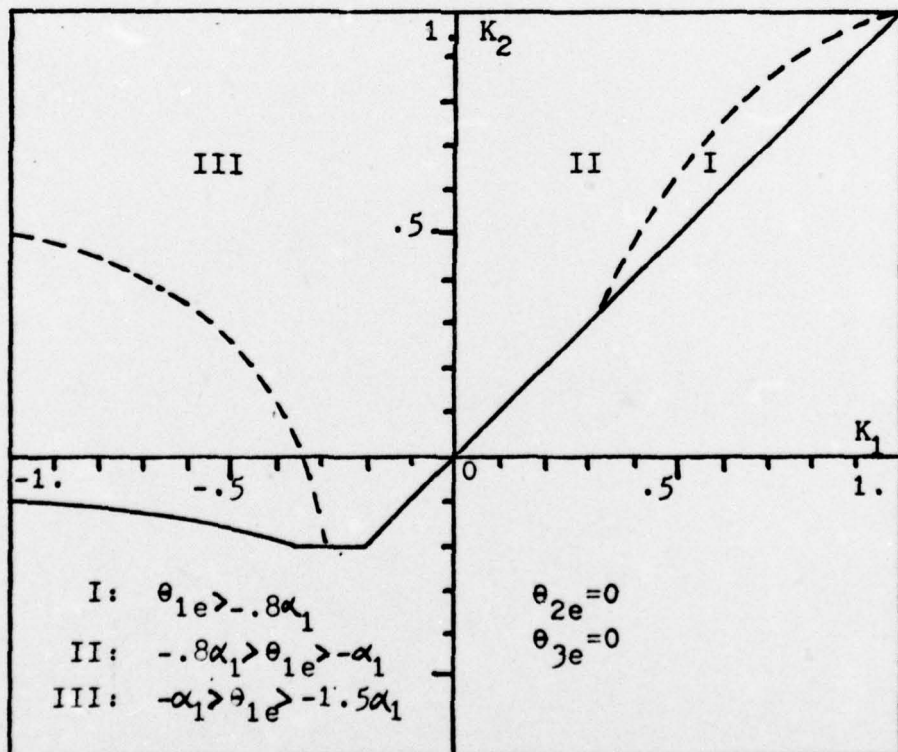
Figure 8.   Stability Region and Equilibrium Angle
Curves: $\alpha_1 = 5^\circ$, $\alpha_2 = 0$, $\beta = 1.$, RA = 0
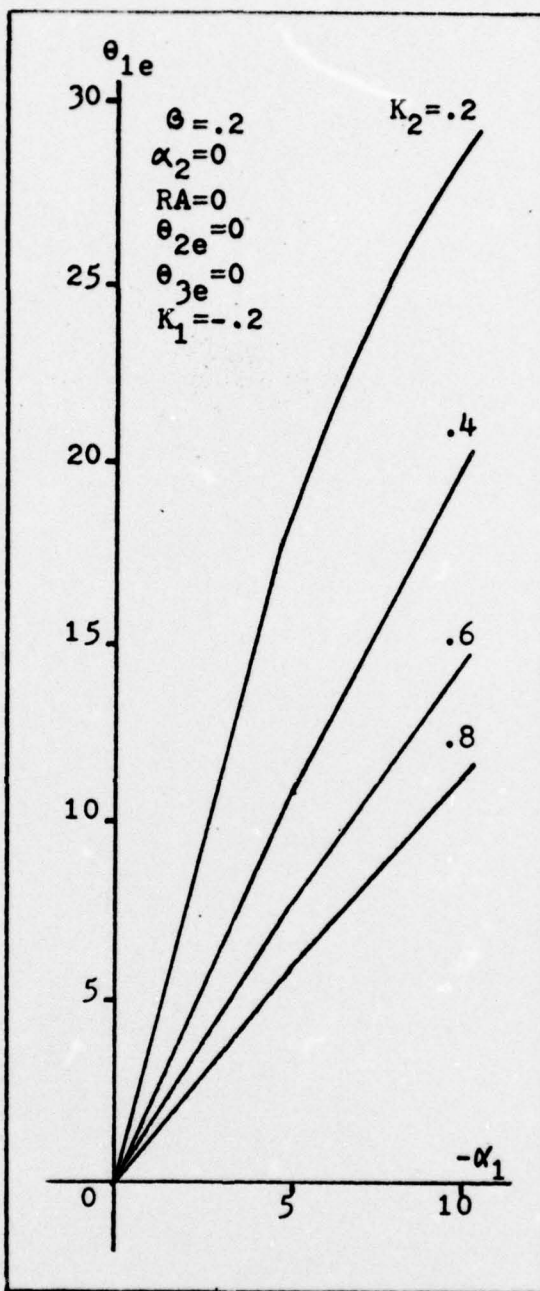
Figure 9. θ_{1e} vs. α_1

linear function of $-\alpha_1$ for any K_2. For $\beta=1$, the region of stability is considerably larger than for $\beta=.2$. With much more angular momentum in the rotor, the equilibrium angles are very much closer to the misalignment angle, $-\alpha_1$.

Presentation of data for misalignment when α_2 is different from zero or $-90°$ is difficult because, in this case, all three Euler angles are different from zero. However, for all stable equilibrium positions which were found, θ_{3e} was always less than $.01°$. Analysis of the numerical data suggest that θ_{1e} is approximately equal to $-\alpha_1 \cos\alpha_2$ when $K_1=0$ or $K_2=1$, and θ_{2e} is approximately equal to $\alpha_1 \sin\alpha_2$ when $K_2=0$. To confirm this observation, it is useful to consider two other relationships between K_1 and K_2, and the equilibrium equations.

$$\frac{C-A}{C} = \frac{K_2(K_1-1)}{K_1 K_2 - 1} \tag{33}$$

$$\frac{C-B}{C} = \frac{K_1(K_2-1)}{K_1 K_2 - 1} \tag{34}$$

$$\frac{(B-A)}{C}[C\theta_1 S2\theta_2 S2\theta_3 - \frac{S2\theta_1}{2}(4S^2\theta_2-1)S^2\theta_3]$$

$$- \frac{(C-B)}{C} S2\theta_1(4S^2\theta_2-1) - \beta[C\theta_1 C\theta_2 S\theta_3 S\alpha_1 S\alpha_2 \tag{35}$$

$$- C\theta_1 C\theta_2 C\theta_3 S\alpha_1 C\alpha_2 - S\theta_1 C\theta_2 C\alpha_1] = 0$$

$$2\frac{(B-A)}{C}[S\theta_1 C2\theta_2 S2\theta_3 + S2\theta_2(C^2\theta_3 - S^2\theta_1 S^2\theta_3)]$$

$$+2\frac{(C-B)}{C}C^2\theta_1 S2\theta_2 - \beta[(C\theta_2 C\theta_3 - S\theta_1 S\theta_2 S\theta_3)S\alpha_1 S\alpha_2 \tag{36}$$

$$(C\theta_2 S\theta_3 + S\theta_1 S\theta_2 S\theta_3)S\alpha_1 C\alpha_2 - C\theta_1 S\theta_2 C\alpha_1] = 0$$

24

Let $\theta_{3e}=0$ and $(C-B)/C=0$, then eqn (35) becomes

$$C\theta_1 C\theta_2 S\alpha_1 C\alpha_2 + S\theta_1 C\theta_2 C\alpha_1 = 0 \qquad (37)$$

which, for small α_1 and θ_{1e}, reduces to

$$\theta_{1e} = -\alpha_1 C\alpha_2 \qquad (38)$$

Also, letting $\theta_{3e}=0$, $(C-A)/C=0$, and θ_{1e} be small, eqn (36) becomes

$$C\theta_2 S\alpha_1 S\alpha_2 - C\theta_1 S\theta_2 C\alpha_1 = 0 \qquad (39)$$

which reduces to

$$\theta_{2e} \approx \alpha_1 S\alpha_2 \qquad (40)$$

Therefore, when α_2 is different from zero or -90° and $\beta=.2$, θ_{1e} is determined from fig. 5 or 6, and θ_{2e} is determined from fig. 7; θ_{3e} is assumed approximately equal to zero. To determine θ_{1e} from fig. 5 or 6, replace α_1 by $\alpha_1 \cos\alpha_2$ in the legend for I, II, and III. To determine θ_{2e} from fig. 7, replace α_1 by $-\alpha_1 \sin\alpha_2$. These approximations are within five percent of the numerical data.

Example II. The second case considered a satellite with no rotor misalignment but a misalignment HZ in the z-direction. The specific purpose of this example was to determine if a misalignment out of the xy-plane could cause instability. For this example HZ was varied from zero to one for HX=.2, $\beta=.2$, RA=.25, and $\lambda^2/\omega_0^2=.1133$. Cases for HX=.5, RA=.5, and $\lambda^2/\omega_0^2=.2267$ were also studied. Table I shows that for HZ=0

25

the satellite was stable about the nominal position where all angles were equal to zero. As HZ was increased to one, ϕ_1 and ϕ_2 increased significantly; however, θ_{1e}, θ_{2e}, and θ_{3e} did not change from zero, i.e., the body orientation remained the same, but the antennas are no longer stable in an equilibrium position of zero energy in the springs. For HZ$\neq$0, ϕ_1 and ϕ_2 are found in Table I, and the stability region for the body is found in fig. 5 (the nominal stability region).

α_1	α_2	HX	HZ	RA	λ^2/ω_o^2	1	2
0	0	.2	0	.25	.1133	0	0
0	0	.2	.1	.25	.1133	4.74	1.09
0	0	.2	.5	.25	.1133	23.74	5.99
0	0	.2	1.0	.25	.1133	46.88	16.13
0	0	.2	.5	.5	.1133	23.75	6.00
5	0	.2	0	.25	.1133	0	0
5	0	.2	.1	.25	.1133	4.74--4.53	1.08--1.19
5	0	.2	.5	.25	.1133	23.74-23.08	6.00--6.42
5	0	.2	1.0	.25	.1133	46.87-45.13	16.13-16.46
5	0	.2	.5	.5	.1133	23.74-22.90	6.00--6.40
5	0	.2	.5	.5	.2267	21.90-21.00	8.18--8.47
5	5	.2	0	.25	.1133	0	0
5	5	.2	.1	.25	.1133	4.75--4.53	1.09--1.19
5	5	.2	.5	.25	.1133	23.74-22.78	5.99--6.42
5	5	.2	1.0	.25	.1133	46.87-45.17	16.13-16.46
5	5	.2	.5	.5	.1133	23.47-22.70	6.00--6.51
10	0	.2	.5	.5	.2267	21.90-20.70	8.18--8.54

Table I. Ranges of ϕ_1 and ϕ_2

θ=.2 for all values in this table

Example III. As shown in Table I, when HZ=0, $\phi_1=\phi_2=0$ is still a stable equilibrium position. The numerical data also showed that the body equilibrium angles did not change from those without the antennas. Therefore, fig. 5, 6, 7, and 8 can be used to determine stability regions and equilibrium angle curves for the satellite with or without antennas

provided HZ=0. When HZ≠0, the body equilibrium angles were reduced. As HZ was increased the stable equilibrium angle curves shifted to the left as indicated in fig. 10. Also as RA was increased to .5, the equilibrium angle curves again shifted slightly to the left as indicated in fig. 11. Doubling the value of λ^2/ω_0^2 did not have significant effect on the body equilibrium angles, but ϕ_1 was reduced by about 8%, and ϕ_2 was increased by about 30%. ϕ_1 and ϕ_2 were very weak functions of K_1 and K_2, and Table I shows the range through which ϕ_1 and ϕ_2 varied as K_1 and K_2 were varied.

Conclusions

Fig. 5, 6, and 8 clearly indicate that if the satellite is designed for stability about the major principal axis, rotor misalignment has much less effect on the equilibrium angle than if designed for the region where K_1 is less than zero. In this case, the equilibrium angle is always less than the misalignment angle. If stability is designed for the region between the nominal equilibrium curve and region III, very minor misalignment of the rotor can cause significant changes in the equilibrium angles. For misalignment in the antennas, the conclusions are not so clearly defined because the specific model was very restricted. For this model, the misalignment actually reduced the body equilibrium angles if there was a rotor misalignment, and had no effect if there was no rotor misalignment. It was tacitly assumed that the antenna equilibrium angles were not important to the actual use of the antenna.

27
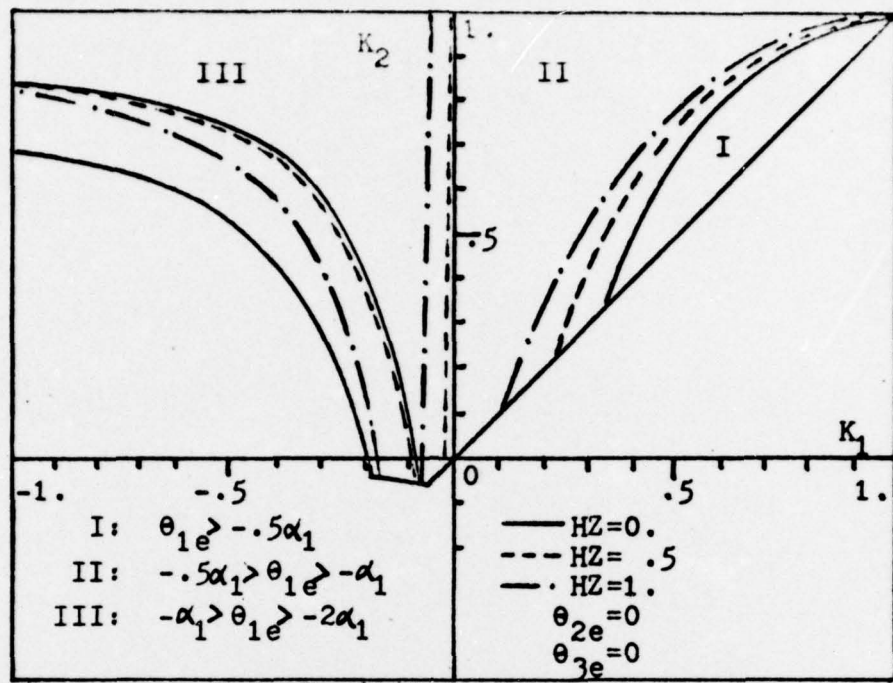
Figure 10. Body Equilibrium Angle Comparison for Changes in HZ

$\alpha_1 = 5^\circ$, $\alpha_2 = 0$, $\beta = .2$, HX=.5, RA=.25, $\lambda^2/\omega_o^2 = .1133$

I: $\theta_{1e} > -.5\alpha_1$

II: $-.5\alpha_1 > \theta_{1e} > -\alpha_1$

III: $-\alpha_1 > \theta_{1e} > -2\alpha_1$

HZ=0.
HZ= .5
HZ=1.
$\theta_{2e}=0$
$\theta_{3e}=0$
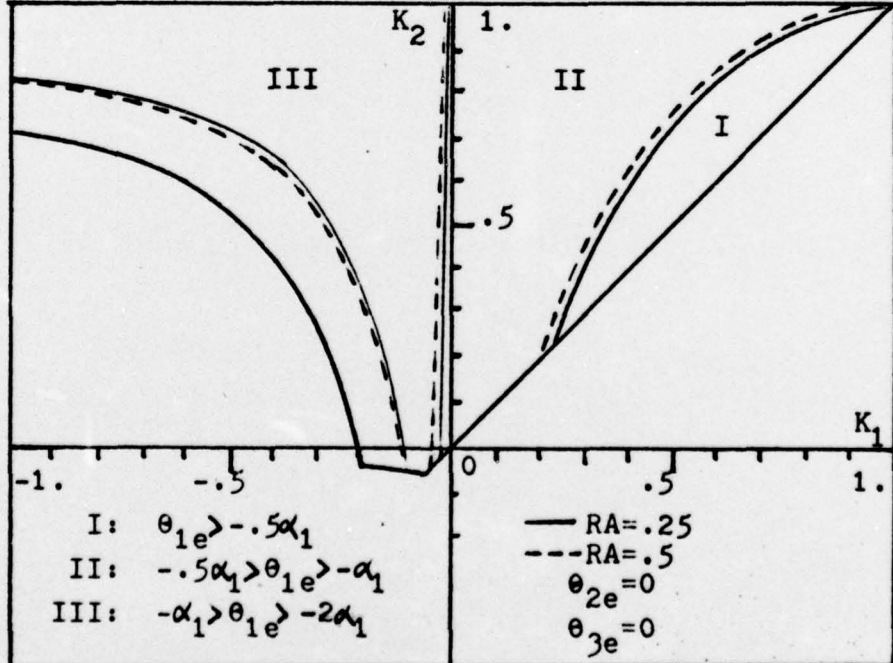
Figure 11. Body Equilibrium Angle Comparison for Changes in RA

$\alpha_1 = 5^\circ$, $\alpha_2 = 0$, $\beta = .2$, HX=.2, HZ=.5, $\lambda^2/\omega_o^2 = .1133$

I: $\theta_{1e} > -.5\alpha_1$

II: $-.5\alpha_1 > \theta_{1e} > -\alpha_1$

III: $-\alpha_1 > \theta_{1e} > -2\alpha_1$

RA=.25
RA=.5
$\theta_{2e}=0$
$\theta_{3e}=0$

28

The theory presented is valid for more general, less restricted antenna models. For instance, misalignments other than HZ, asymmetric motion, or motion in the xy-plane could be allowed. To do this, one would only have to redefine the inertia matrices of the antennas.

Bibliography

1. Pringle, R. Jr., "On the Stability of a Body with Connected Moving Parts," _AIAA Journal_, Vol. 4, No. 8, 1966, 1395-1404.

2. Meirovitch, L. and Nelson, H.D., "On the High-Spin Motion of a Satellite Containing Elastic Parts," _Journal of Spacecraft and Rockets_, Vol. 3, No. 11, 1966, 1597-1602.

3. Nelson, H.D. and Meirovitch, L., "Stability of a Nonsymmetrical Satellite with Elastically Connected Moving Parts," _The Journal of the Astronautical Sciences_, Vol. 13, No. 6, 226-234.

4. Likins, P.W., "Attitude Stability of Dual-Spin Systems," _Hughes Aircraft Company, Space Systems Divisions Report_, SSD 60377R, September 1966.

5. Crespo da Silva, M.R.M., "Attitude Stability of a Gravity-Stabilized Gyrostat Satellite," _Celestial Mechanics_, Vol. 2, 1970, 147-165.

6. Rumiantsev, V.V., "On the Stability of Stationary Motions of the Gyrostat Satellite," _18th Congress of the International Astronautical Federation_, Belgrade, 1967.

7. Meirovitch, L. and Calico, R.A., "The Stability of Motion of Satellites with Flexible Appendages," _NASA Contractor Report_, NASA CR-1978, February 1972.

8. Calico, R.A., "Stability of a Gyrostat Satellite with Flexible Appendages," _Journal of Spacecraft and Rockets_, Vol. 13, No. 8, August 1976, 505-508.

9. Calico, R.A., "Stability of a Flexible Satellite Containing Internal Rotors," _AIAA Paper 76-786_, AIAA/AAS Astrodynamics Conference, San Diego, California, August 1976.

10. Meirovitch, L., _Methods of Analytical Dynamics_, McGraw-Hill Book Co, N.Y., 1970.

Appendix A

Kinetic Energy Derivation

The kinetic energy of a body may be written as

$$T = \frac{1}{2} \int_m \{\dot{R}\}^T \{\dot{R}\} \, dm \qquad (5)$$

If $\{\dot{R}\} = \{\dot{R}_c\} + \{\dot{r}\}$, then eqn (5) becomes

$$T = \frac{1}{2} m \{\dot{R}_c\}^T \{\dot{R}_o\} + \frac{1}{2} \int_m \{\dot{r}\}^T \{\dot{r}\} \, dm + \{\dot{R}_c\}^T \int_m \{\dot{r}\} \, dm \qquad (41)$$

By definition of the center of mass $\int_m \{r\} dm = 0$, and the last term in eqn (41) is identically zero. There are several distinct domains in the body, and the second term in eqn (41) is more easily calculated by integrating over each domain and summing over the entire body.

Considering the rigid portion first, $\underline{\dot{r}} = \underline{\omega} \times \underline{r}_o$ because $\underline{\dot{r}}_o' = 0$. Therefore

$$\frac{1}{2} \int_{m_o} \{\dot{r}\}^T \{\dot{r}\} \, dm_o = \frac{1}{2} \{\omega\}^T \int_{m_o} \{r_o\}^T \{r_o\} \, dm \, \{\omega\} \qquad (42)$$

$$= \frac{1}{2} \{\omega\}^T [J_o] \{\omega\}$$

For the ith antenna, $\underline{\dot{r}} = \underline{\omega} \times \underline{r}_i + \underline{\dot{r}}_i'$; however $\underline{r}_i = \underline{r}_{oi} + \underline{\rho}_i$. So

$$\underline{\dot{r}} = \underline{\omega} \times (r_{oi} + \underline{\rho}_i) + \dot{\underline{\rho}}_i' \qquad (43)$$

and

$$\frac{1}{2} \int_{m_i} \{\dot{r}\}^T \{\dot{r}\} \, dm_i = \frac{1}{2} \{\omega\}^T \int_{m_i} [l_i]^T [\widetilde{(r_{oi} + \rho_i)}]^T [\widetilde{(r_{oi} + \rho_i)}][l_i] \, dm \, \{\omega\}$$

$$+ \{\omega\}^T \int_{m_i} [\widetilde{(r_{oi} + \rho_i)}][l_i]^T \{\dot{\rho}_i'\} \, dm_i + \frac{1}{2} \int_{m_i} \{\dot{\rho}_i'\}^T \{\dot{\rho}_i'\} \, dm_i$$

$$\qquad (44)$$

31

The first term on the right of the equal sign in eqn (44) reduces to $\frac{1}{2}\{\omega\}^{\mathsf{T}}[\ell_i]^{\mathsf{T}}[J_i][\ell_i]\{\omega\}$.

Similarly for the jth rotor, $\underline{\dot{r}} = \underline{\omega} \times \underline{\dot{r}}'_j$, and $\underline{\dot{r}}'_j = \underline{\Omega}_j \times \underline{\rho}_j$. So

$$\frac{1}{2}\int_{m_j}\{\dot{r}\}^{\mathsf{T}}\{\dot{r}\}dm_j = \frac{1}{2}[\Omega_j]^{\mathsf{T}}[J_j][\Omega_j] + \{\omega\}^{\mathsf{T}}[\ell_j]^{\mathsf{T}}[J_j][\ell_j]\{\omega\} \qquad (45)$$

The part of the kinetic energy of the rotor which does not arise from its spin has been included in $[J_0]$.

Combining eqns (5), (42), (44), and (45) yields the total kinetic energy for the system (eqn (6)).

32

Formulation of $[J_i]_r$ and $[J_i]_e$.

Fig. B-1 shows the model used for the antennas. Since they are symmetrical about the z-axis, and are restricted to motion in the xz-plane, all products of inertia vanish, and I_{yy} is the sum of I_{xx} and I_{zz}. Since the antennas are symmetrical, only one
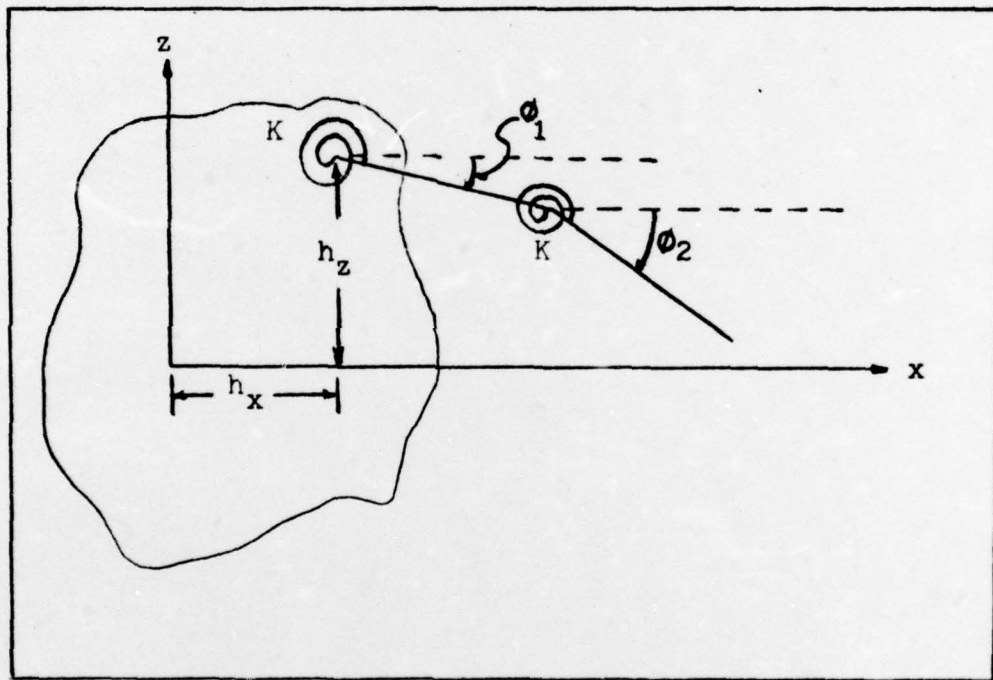

Figure B-1. Antenna model

is shown. From the definition of moments-of-inertia $I_{xx}=2\int_D \mu z^2 dD$; therefore,

$$I_{xx} = 2\int_0^L \mu (h_z - \tau s\phi_1)^2 d\tau + 2\int_L^{2L} \mu (h_z - \tau s\phi_2 - L s\phi_1) d\tau$$

$$= m L^2 (HZ^2 + s^2\phi_1 + \frac{s^2\phi_2}{3} - 2HZ s\phi_1 - HZ s\phi_2 + s\phi_1 s\phi_2)$$

(46)

Also, $I_{zz} = 2\int_D \mu x^2 dD$; therefore,

$$I_{zz} = 2\int_0^L \mu(h_x + \tau c\phi_1)^2 d\tau + 2\int_L^{2L} \mu(h_x + \tau c\phi_2 + Lc\phi_1) d\tau \tag{47}$$

$$= mL^2(HX^2 + c^2\phi_1 + \frac{c^2\phi_2}{3} + 2HXc\phi_1 + HXc\phi_2 + c\phi_1 c\phi_2$$

$[J_i]_r$ consists of those values of I_{xx}, I_{yy}, and I_{zz} evaluated for $\phi_1 = \phi_2 = 0$. $[J_i]_e$ consists of the complete matrix $[I_{ij}]$ less $[J_i]_r$, which yields eqns (21) and (24). It should be noted this inertia matrix for the antennas is valid only for symmetrical motion.

34

Equilibrium Equations and Dynamic Potential

Equilibrium Equations

The following equations were used to determine the equilibrium angles.

$$\frac{\partial U}{\partial \theta_1} = \left(\frac{B'-A'}{C}\right)\left[c\theta_1 \, s2\theta_2 \, s2\theta_3 - \frac{s2\theta_1}{2}(4s^2\theta_2 - 1) s^2\theta_3\right]$$

$$-(c'-B')\frac{s2\theta_1}{2}(4s^2\theta_2 - 1) - \beta[c\theta_1 c\theta_2 s\theta_3 s\alpha_1 s\alpha_2 \qquad (48)$$

$$- c\theta_1 c\theta_2 c\theta_3 s\alpha_1 c\alpha_2 - s\theta_1 c\theta_2 c\alpha_1] = 0$$

$$\frac{\partial U}{\partial \theta_2} = 2\left(\frac{B'-A'}{C}\right)\left[s\theta_1 c2\theta_2 s2\theta_3 + s2\theta_2(c^2\theta_3 - s^2\theta_1 s^2\theta_3)\right]$$

$$+ 2\left(\frac{c'-B'}{C}\right)c^2\theta_1 s2\theta_2 - \beta[(c\theta_2 c\theta_3 - s\theta_1 s\theta_2 s\theta_3)s\alpha_1 s\alpha_2 \qquad (49)$$

$$+ (c\theta_2 s\theta_3 + s\theta_1 s\theta_2 c\theta_3) s\alpha_1 c\alpha_2 - c\theta_1 s\theta_2 c\alpha_1] = 0$$

$$\frac{\partial U}{\partial \theta_3} = \left(\frac{B'-A'}{C}\right)\left[2 s\theta_1 s2\theta_2 c2\theta_3 + \frac{s2\theta_3}{2}(4c^2\theta_2 - 1)\right.$$

$$\left. - \frac{s^2\theta_1}{2} s2\theta_3(4s^2\theta_2 - 1)\right] - \beta[(-s\theta_2 s\theta_3 + s\theta_1 c\theta_2 c\theta_3) s\alpha_1 s\alpha_2$$

$$+ (s\theta_2 c\theta_3 + s\theta_1 c\theta_2 s\theta_3) s\alpha_1 c\alpha_2] = 0 \qquad (50)$$

$$\frac{\partial U}{\partial \phi_1} = \frac{3}{2C} \left[\frac{\partial A'}{\partial \phi_1} (c\theta_2 c\theta_3 - s\theta_1 s\theta_2 s\theta_3)^2 + \frac{\partial B'}{\partial \phi_1} (c\theta_2 s\theta_3 \right.$$

$$+ s\theta_1 s\theta_2 c\theta_3)^2 + \frac{\partial C'}{\partial \phi_1} (c\theta_1 s\theta_2)^2] - \frac{1}{2C} [(s\theta_1 c\theta_3$$

$$+ s\theta_1 c\theta_2 s\theta_3)^2 \frac{\partial A'}{\partial \phi_1} + \frac{\partial B'}{\partial \phi_1} (s\theta_2 s\theta_3 - s\theta_1 c\theta_2 c\theta_3)^2 \quad (51)$$

$$+ \frac{\partial C'}{\partial \phi_1} (c\theta_1 c\theta_2)^2] + \frac{K}{C} (2\phi_1 - \phi_2) = 0$$

$$\frac{\partial U}{\partial \phi_2} = \frac{3}{2C} \left[\frac{\partial A'}{\partial \phi_2} (c\theta_2 c\theta_3 - s\theta_1 s\theta_2 s\theta_3)^2 + \frac{\partial B'}{\partial \phi_2} (c\theta_2 s\theta_3 \right.$$

$$+ s\theta_1 s\theta_2 c\theta_3)^2 + \frac{\partial C'}{\partial \phi_2} (c\theta_1 s\theta_2)^2] - \frac{1}{2C} [\frac{\partial A'}{\partial \phi_2} (s\theta_2 c\theta_3$$

$$+ s\theta_1 c\theta_2 s\theta_3)^2 + \frac{\partial B'}{\partial \phi_2} (s\theta_2 s\theta_3 - s\theta_1 c\theta_2 c\theta_3)^2 \quad (52)$$

$$+ \frac{\partial C'}{\partial \phi_2} (c\theta_1 c\theta_2)^2] + \frac{K}{C} (\phi_2 - \phi_1) = 0$$

where

$$A' = A + mL^2 I_{1e}, \quad B' = B + mL^2 I_{2e}, \quad C' = B + mL^2 I_{3e} \quad (53)$$

and

$$\frac{\partial A'}{\partial \phi_1} = mL^2 (2s2\phi_1 + c\phi_1 s\phi_2 - 2HZ c\phi_1)$$

$$\frac{\partial B'}{\partial \phi_1} = mL^2 (- HZ c\phi_1 + c\phi_1 s\phi_2 - s\phi_1 c\phi_2 - 2HX s\phi_1) \quad (54)$$

$$\frac{\partial C'}{\partial \phi_1} = mL^2 (- 2s2\phi_1 - 2HX s\phi_1 - s\phi_1 c\phi_2)$$

36

and

$$\frac{\partial A'}{\partial \phi_2} = mL^2 \left(\frac{2S2\theta_2}{3} - HZC\phi_2 + S\phi_1 C\phi_2 \right)$$

$$\frac{\partial B'}{\partial \phi_2} = mL^2 \left(-HZC\phi_2 + S\phi_1 C\phi_2 - HXC\phi_2 - C\phi_1 S\phi_2 \right) \tag{55}$$

$$\frac{\partial C'}{\partial \phi_2} = mL^2 \left(-\frac{2S2\theta_2}{3} - C\phi_1 S\phi_2 - HXC\phi_2 \right)$$

Dynamic Potential

The following equations are the dynamic potential used to formulate $[U_{ij}]$ and determine its sign definiteness.

$$U_{11} = \frac{(B'-A')}{C} \left[-S\theta_1 S2\theta_2 S2\theta_3 - C2\theta_1 (4S^2\theta_2 - 1)S^2\theta_3 \right]$$

$$- \frac{(C'-B')}{C} \left[C2\theta_1 (4S^2\theta_2 - 1) \right] - \beta \left[-S\theta_1 C\theta_2 S\theta_3 S\alpha_1 S\alpha_2 \right. \tag{56}$$

$$\left. + S\theta_1 C\theta_2 C\theta_3 S\alpha_1 C\alpha_2 - C\theta_1 C\theta_2 C\alpha_1 \right]$$

$$U_{12} = \frac{(B'-A')}{C} \left(2C\theta_1 C2\theta_2 S2\theta_3 - 2S2\theta_1 S2\theta_2 S^2\theta_3 \right)$$

$$- \frac{(C'-A')}{C} \left(2S2\theta_1 S2\theta_2 \right) - \beta \left[-C\theta_1 S\theta_2 S\theta_3 S\alpha_1 S\alpha_2 \right. \tag{57}$$

$$\left. + C\theta_1 S\theta_2 C\theta_3 S\alpha_1 C\alpha_2 + S\theta_1 S\theta_2 C\alpha_1 \right]$$

$$U_{13} = \frac{(B'-A')}{C} \left[2C\theta_1 S2\theta_2 C2\theta_3 - \frac{S2\theta_1}{2} (4S^2\theta_2 - 1)S^2\theta_3 \right]$$

$$- \beta \left(C\theta_1 C\theta_2 C\theta_3 S\alpha_1 S\alpha_2 + C\theta_1 C\theta_2 S\theta_3 S\alpha_1 C\alpha_2 \right) \tag{58}$$

37

$$U_{14} = \frac{\partial C'}{\partial \phi_1} \frac{1}{C} \left[C\theta_1 S2\theta_2 S2\theta_3 - \frac{S2\theta_1}{2} (4S^2\theta_2 - 1) S^2\theta_3 \right]$$
$$- \frac{1}{C} \frac{\partial A'}{\partial \phi_1} \left[\frac{S2\theta_1}{2} (4S^2\theta_2 - 1) \right] \tag{59}$$

$$U_{15} = \frac{1}{C} \frac{\partial C'}{\partial \phi_2} \left[C\theta_1 S2\theta_2 S2\theta_3 - \frac{S2\theta_1}{2} (4S^2\theta_2 - 1) S^2\theta_3 \right]$$
$$- \frac{1}{C} \frac{\partial A'}{\partial \phi_2} \left[\frac{S2\theta_1}{2} (4S^2\theta_2 - 1) \right] \tag{60}$$

$$U_{22} = \frac{4}{C} (B' - A') \left[-S\theta_1 S2\theta_2 S2\theta_3 + C2\theta_2 (C^2\theta_3 - S^2\theta_1 S^2\theta_3) \right]$$
$$+ \frac{4}{C} (C' - A') C^2\theta_1 C2\theta_2 - \beta \left[-S\theta_2 C\theta_3 - S\theta_1 C\theta_2 S\theta_3 \right) S\alpha_1 S\alpha_2$$
$$+ (-S\theta_2 S\theta_3 + S\theta_1 C\theta_2 C\theta_3) S\alpha_1 C\alpha_2 - C\theta_1 C\theta_2 C\alpha_2 \right] \tag{61}$$

$$U_{23} = \frac{2}{C} (B' - A') \left[2 S\theta_1 C2\theta_2 C2\theta_3 - S2\theta_2 S2\theta_3 (1 + S^2\theta_1) \right]$$
$$- \beta \left[(-C\theta_2 S\theta_2 - S\theta_1 S\theta_2 C\theta_3) S\alpha_1 S\alpha_2 + (C\theta_2 C\theta_2 \right.$$
$$\left. - S\theta_1 S\theta_2 S\theta_3) S\alpha_1 C\alpha_2 \right] \tag{62}$$

$$U_{24} = \frac{2}{C} \frac{\partial C'}{\partial \phi_1} \left[S\theta_1 C2\theta_2 S2\theta_3 + S2\theta_2 (C^2\theta_3 - S^2\theta_1 S^2\theta_3) \right]$$
$$+ \frac{2}{C} \frac{\partial A'}{\partial \phi_1} C^2\theta_1 S2\theta_2 \tag{63}$$

38

$$U_{25} = \frac{2}{c} \frac{\partial C'}{\partial \phi_2} \left[S\theta_1 C2\theta_2 S2\theta_3 + S2\theta_2 (c^2\theta_3 - s^2\theta_1 s^2\theta_3) \right.$$

$$\left. + \frac{2}{c} \frac{\partial A'}{\partial \phi_2} c^2\theta_1 S2\theta_2 \right. \tag{64}$$

$$U_{33} = \frac{1}{c} (B - A')[-4S\theta_1 S2\theta_2 S2\theta_3 + C2\theta_3(4c^2\theta_2 - 1)$$

$$-s^2\theta_1 (4s^2\theta_2 - 1) C2\theta_3] - \beta[(-S\theta_2 C\theta_3 - S\theta_1 C\theta_2 S\theta_3) S\alpha_1 S\alpha_2$$

$$+ (-S\theta_2 S\theta_3 + S\theta_1 C\theta_2 C\theta_3) S\alpha_1 C\alpha_2] \tag{65}$$

$$U_{34} = \frac{1}{c} \frac{\partial C'}{\partial \phi_1} \left[2 S\theta_1 S2\theta_2 C2\theta_3 + \frac{S2\theta_3}{2} (4c^2\theta_2 - 1) \right.$$

$$\left. - \frac{s^2\theta_1}{2} S2\theta_3 (4s^2\theta_2 - 1) \right] \tag{66}$$

$$U_{35} = \frac{1}{c} \frac{\partial C'}{\partial \phi_2} \left[2 S\theta_1 S2\theta_2 C2\theta_3 + \frac{S2\theta_3}{2} (4c^2\theta_2 - 1) \right.$$

$$\left. - \frac{s^2\theta_1}{2} S2\theta_3 (4s^2\theta_2 - 1) \right] \tag{67}$$

$$U_{44} = \frac{3}{2c} \left[\frac{\partial^2 A'}{\partial \phi_1^2} (C\theta_2 C\theta_3 - S\theta_1 S\theta_2 S\theta_3)^2 + \frac{\partial^2 B'}{\partial \phi_1^2} (C\theta_2 S\theta_3 \right.$$

$$+ S\theta_1 S\theta_2 C\theta_3)^2 + \frac{\partial^2 C'}{\partial \phi_1^2} (C\theta_1 S\theta_2)^2 \right] - \frac{1}{2c} \left[\frac{\partial^2 A'}{\partial \phi_1^2} (S\theta_2 C\theta_3 \right.$$

$$+ S\theta_1 C\theta_2 S\theta_3)^2 + \frac{\partial^2 B'}{\partial \phi_1^2} (S\theta_2 S\theta_3 - S\theta_1 C\theta_2 C\theta_3)^2 \tag{68}$$

$$+ \frac{\partial^2 C'}{\partial \phi_1^2} (C\theta_1 C\theta_2)^2 \right] + \frac{2K}{c}$$

39

$$U_{4S} = \frac{3}{2C} \left[\frac{\partial^2 A'}{\partial \theta_1 \partial \phi_2} (C\theta_2 C\theta_3 - S\theta_1 S\theta_2 S\theta_3)^2 + \frac{\partial^2 B'}{\partial \phi_1 \partial \phi_2} (C\theta_2 S\theta_3 \right.$$

$$\left. + S\theta_1 S\theta_2 C\theta_3)^2 + \frac{\partial^2 C'}{\partial \phi_1 \partial \phi_2} (C\theta_1 S\theta_2)^2 \right] - \frac{1}{2C} \left[\frac{\partial^2 A'}{\partial \phi_1 \partial \phi_2} (S\theta_2 C\theta_3 \right.$$

$$+ S\theta_1 C\theta_2 S\theta_3)^2 + \frac{\partial^2 B'}{\partial \phi_1 \partial \phi_2} (S\theta_2 S\theta_3 - S\theta_1 C\theta_2 C\theta_3)^2$$

$$\left. + \frac{\partial^2 C'}{\partial \phi_1 \partial \phi_2} (C\theta_1 C\theta_2)^2 - \frac{K}{C} \right. \tag{69}$$

$$U_{SS} = \frac{3}{2C} \left[\frac{\partial^2 A'}{\partial \phi_2^2} (C\theta_2 C\theta_3 - S\theta_1 S\theta_2 S\theta_3)^2 + \frac{\partial^2 B'}{\partial \phi_2^2} (C\theta_2 S\theta_3 \right.$$

$$+ S\theta_1 S\theta_2 C\theta_3)^2 + \frac{\partial^2 C'}{\partial \phi_2^2} (C\theta_1 S\theta_2)^2 - \frac{1}{2C} \left[\frac{\partial^2 A'}{\partial \phi_2^2} (S\theta_2 C\theta_3 \right.$$

$$+ S\theta_1 C\theta_2 S\theta_3)^2 + \frac{\partial^2 B'}{\partial \phi_2^2} (S\theta_2 S\theta_3 - S\theta_1 C\theta_2 C\theta_3)^2$$

$$\left. + \frac{\partial^2 C'}{\partial \phi_2^2} (C\theta_1 C\theta_2)^2 + \frac{K}{C} \right. \tag{70}$$

where

$$\frac{\partial^2 A'}{\partial \phi_1^2} = mL^2 (4c2\phi_1 - S\phi_1 S\phi_2 + 2HZ S\phi_1)$$

$$\frac{\partial^2 B'}{\partial \phi_1^2} = mL^2 (HZ S\phi_1 - S\phi_1 S\phi_2 - C\phi_1 C\phi_2 - 2HX C\phi_1)$$

$$\frac{\partial^2 C'}{\partial \phi_1} = mL^2 (-4S2\phi_1 - 2HX C\phi_1 - C\phi_1 C\phi_2) \tag{71}$$

$$\frac{\partial^2 A'}{\partial \phi_1 \partial \phi_2} = mL^2 C\phi_1 C\phi_2$$

$$\frac{\partial^2 B'}{\partial \phi_1 \partial \phi_2} = mL^2 (C\phi_1 C\phi_2 + S\phi_1 S\phi_2)$$

$$\frac{\partial^2 C'}{\partial \phi_1 \partial \phi_2} = -mL^2 S\phi_1 S\phi_2$$

$$\frac{\partial^2 A'}{\partial \phi_2^2} = mL^2 \left(\frac{4}{3} C2\phi_2 + HZ S\phi_2 - S\phi_1 S\phi_2 \right)$$

$$\frac{\partial^2 B'}{\partial \phi_2^2} = mL^2 \left(HZ S\phi_2 - S\phi_1 S\phi_2 + HX S\phi_2 - C\phi_1 C\phi_2 \right) \qquad (70)$$

$$\frac{\partial^2 C'}{\partial \phi_2^2} = mL^2 \left(-\frac{4}{3} C2\phi_2 - C\phi_1 C\phi_2 + HX S\phi_2 \right)$$

VITA

Phillip Eugene Sanders was born on 13 November 1941 in
Neosho, Missouri. He graduated from John Swett High School,
Crockett, California in 1959 and subsequently enlisted in the
Air Force in April 1960. As an enlisted member, he studied
Chinese language at Yale University and had tours of duty in
Okinawa, Japan, and California. He entered the Airman Education
and Commissioning Program in 1965 and graduated from Arizona
State University in 1967 with a Bachelor of Science in Engineer-
ing (ME) degree. He was a distinguished graduate of OTS. He
completed pilot training and received his wings in October
1968. He flew the F-105D at Tahkli, Thailand in 1969-1970.
He flew the A-7D at Myrtle Beach AFB, South Carolina from 1971-
1975. His last tour included a six-month tour at Korat, Thai-
land in 1972. He entered the School of Engineering, Air
Force Institute of Technology in June 1975.

        Permanant address: 13613 San Pablo Ave.
                             San Pablo, California 94803

REPORT DOCUMENTATION PAGE		READ INSTRUCTIONS BEFORE COMPLETING FORM
1. REPORT NUMBER GA/MC/76D-13 ✓	2. GOVT ACCESSION NO.	3. RECIPIENT'S CATALOG NUMBER
4. TITLE (and Subtitle) ATTITUDE STABILITY OF AN ORBITING SATELLITE CONTAINING FLEXIBLE ANTENNAS AND SPINNING ROTORS ✓		5. TYPE OF REPORT & PERIOD COVERED MS Thesis
		6. PERFORMING ORG. REPORT NUMBER
7. AUTHOR(s) Phillip E. Sanders		8. CONTRACT OR GRANT NUMBER(s)
9. PERFORMING ORGANIZATION NAME AND ADDRESS Air Force Institute of Technology (AFIT-EN) Wright-Patterson AFB, Ohio 45433 ✓		10. PROGRAM ELEMENT, PROJECT, TASK AREA & WORK UNIT NUMBERS
11. CONTROLLING OFFICE NAME AND ADDRESS		12. REPORT DATE December 1976
		13. NUMBER OF PAGES 49
14. MONITORING AGENCY NAME & ADDRESS(if different from Controlling Office)		15. SECURITY CLASS. (of this report) Unclassified
		15a. DECLASSIFICATION/DOWNGRADING SCHEDULE

16. DISTRIBUTION STATEMENT (of this Report)

Approved for public release; distribution unlimited.

17. DISTRIBUTION STATEMENT (of the abstract entered in Block 20, if different from Report)

18. SUPPLEMENTARY NOTES

Approved for public release; IAW AFR 190-17

JERRAL F. GUESS, Captain, USAF
Director of Information

19. KEY WORDS (Continue on reverse side if necessary and identify by block number)

Gyrostat Satellite
Gravity stabilized
Flexible Antennas

20. ABSTRACT (Continue on reverse side if necessary and identify by block number)

This study considers the attitude stability of a gyrostat satellite containing flexible antennas, in which any, or all, of the rotors or antennas may be misaligned with the main body principal axes. The problem is formulated in general for any number of rigid, symmetrical, spinning rotors which are fixed relative to the body and for any number of antennas, modeled as rigid rods connected by torsional springs. The stability analysis is based on the Liapunov direct method, using the Hamiltonian as the Liapunov function. Examples are presented for a gravity-stabilized satellite containing one ⟶ next page

DD FORM 1473 1 JAN 73   EDITION OF 1 NOV 65 IS OBSOLETE

cont

constant-speed rotor and two antennas of two rods each. The antenna misalignment and motion is restricted to the xz-plane. Results show that for a rotor misalignment, the largest deviation from the position defined by the body principal axes aligning with the orbital axes occurs when the misalignment is toward the orbit tangent. Misalignment of the antennas has no effect on the body equilibrium position except when the rotor was also misaligned. In that case, the body equilibrium angles were reduced.